

Compact Objects in Brans-Dick Gravity

Speaker: Amal Majid

Supervisor: Prof. Dr. Muhammad Sharif

University of the Punjab

1st International Electronic Conference on Universe



Stellar Evolution

From Beginning till End

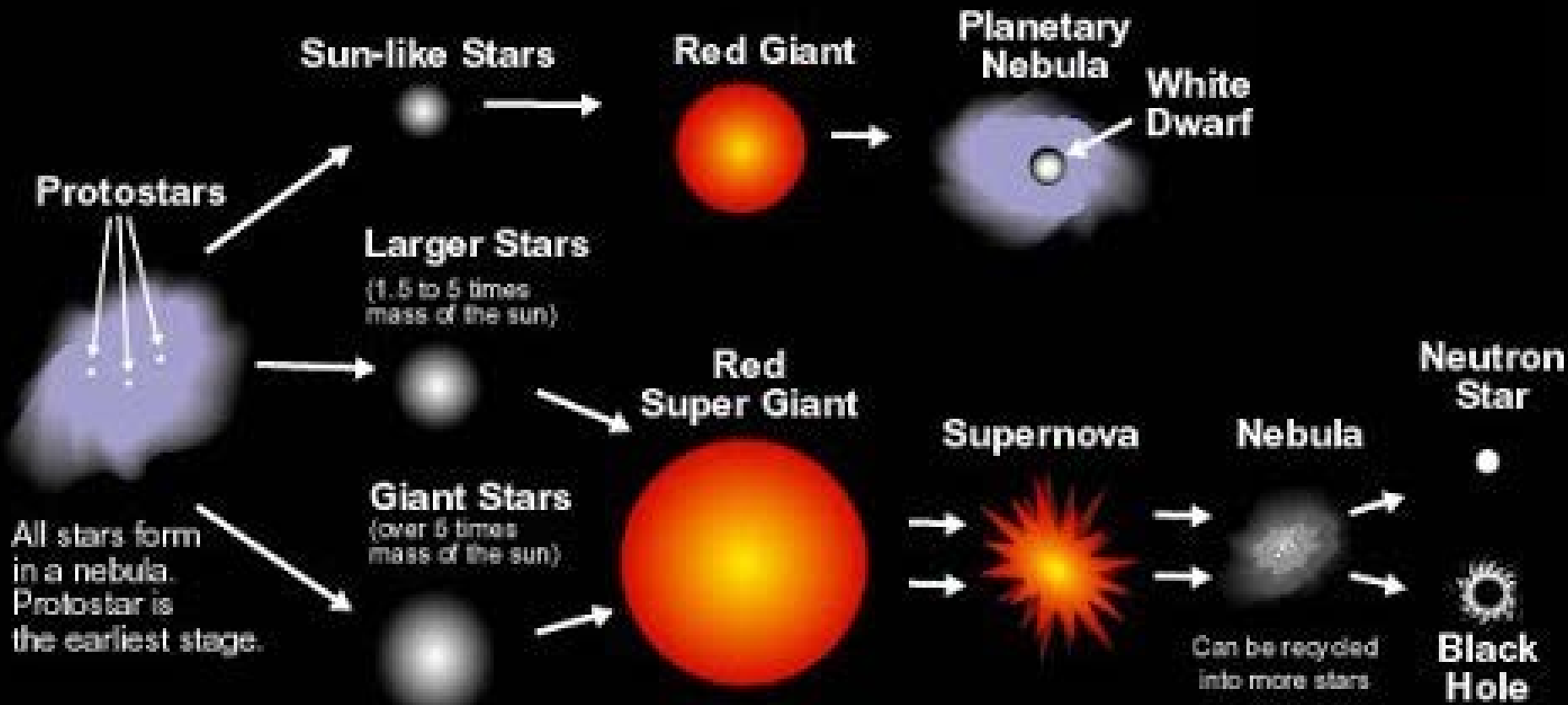
BIRTH

MAIN SEQUENCE

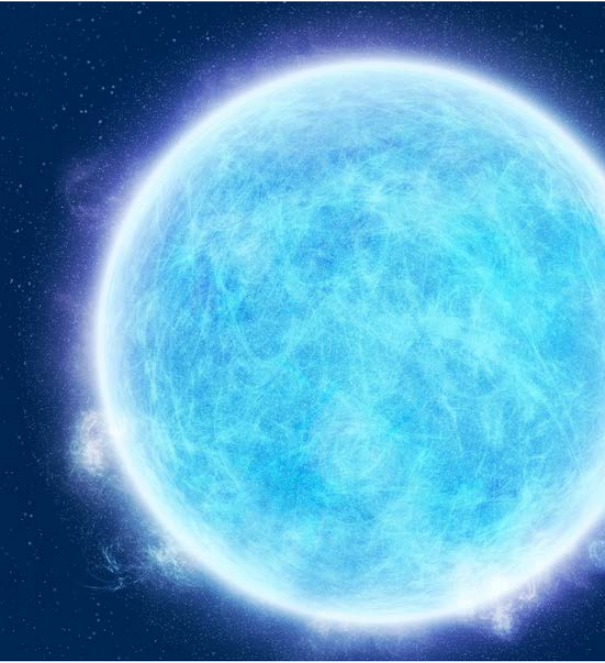
OLD AGE

DEATH

REMNANTS



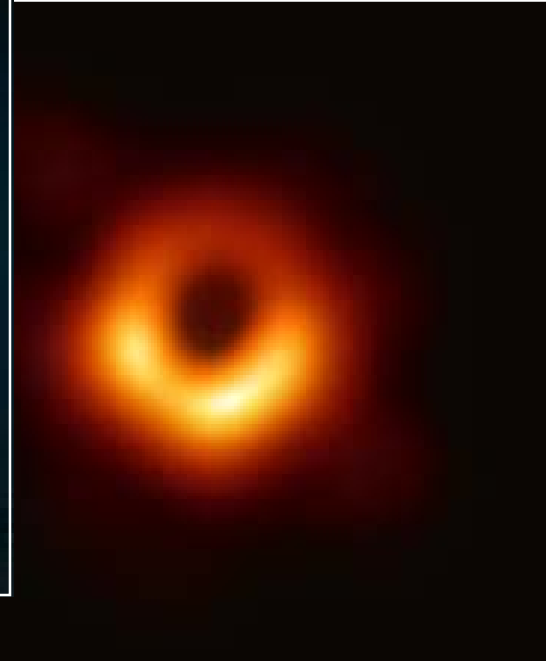
Compact Objects



White Dwarf



Neutron Star



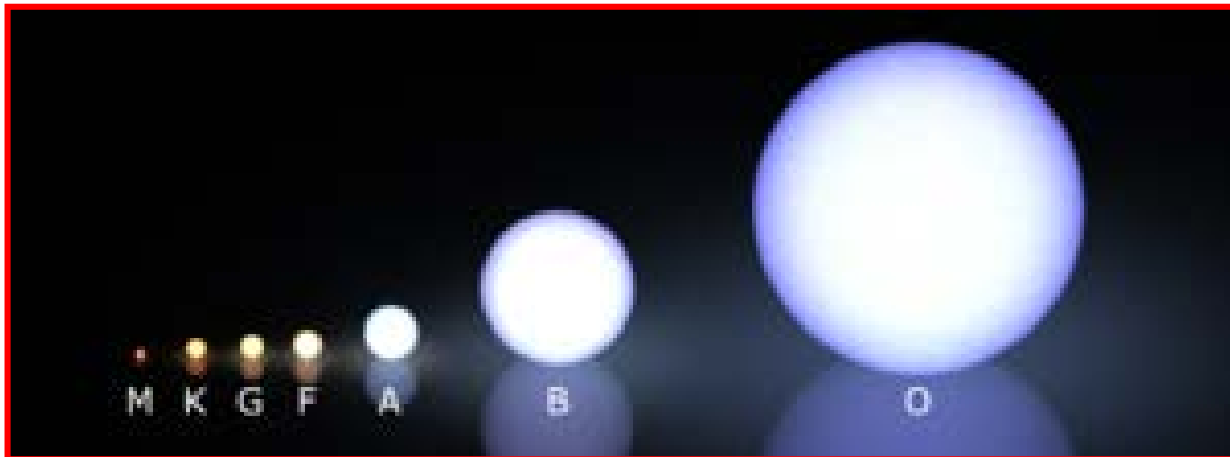
Black Hole

Collapse of a Star → **Compact Objects**

Classification

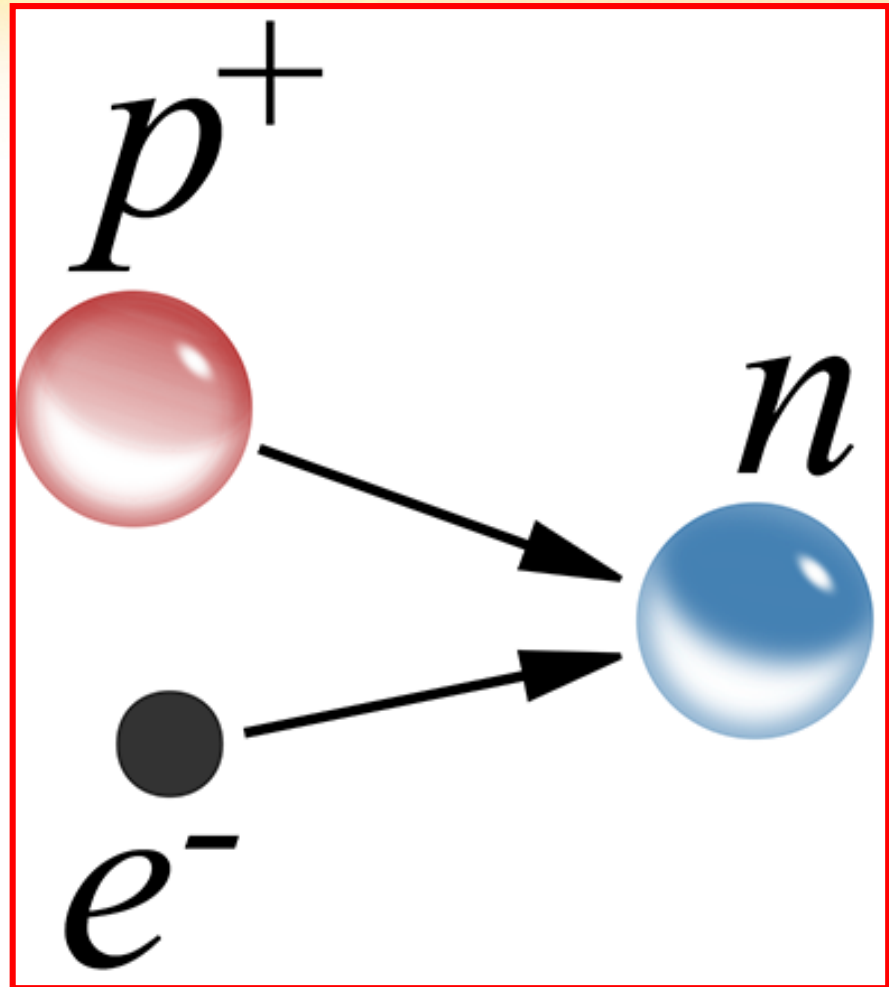
Stars are classified by:

- size
- mass
- luminosity
- colour



Neutron Star

If the collapsing stellar core at the center of a supernova contains between **1.5 and 3 solar masses**, the collapse continues until **electrons and protons combine to form neutrons**, producing a neutron star.



- Gravitational pull is balanced by **neutron degeneracy pressure**.
- Most dense object after the black hole.
- A **cubic meter** of a neutron star would weigh around **400 billion tonnes**.



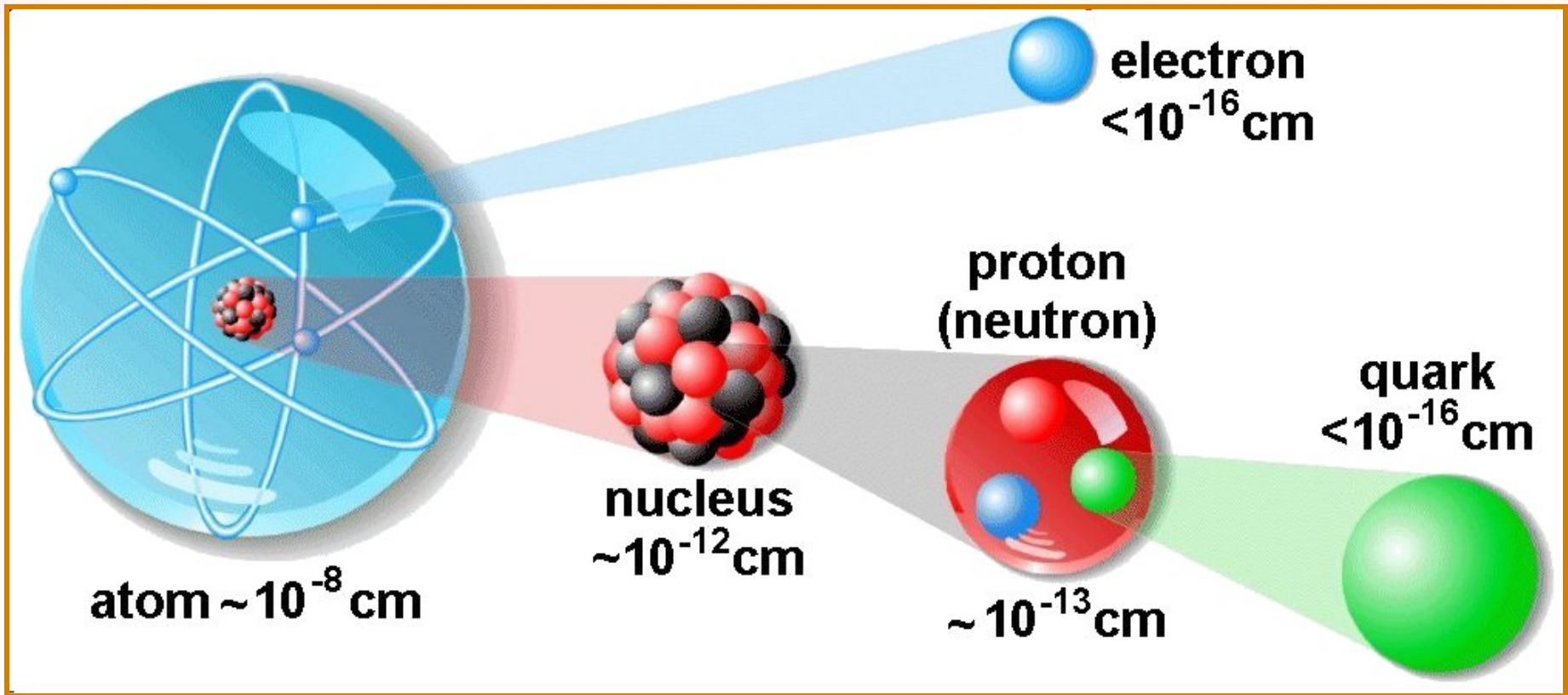
Link to Early Universe

The detection of **strontium** in **GW170817** merger suggests the presence of **heavier elements** within neutron stars. Thus, **cores of neutron or quark stars are like fossils** which allow us to peek back in time to the beginning of everything.

Quark Matter

The environment in the **core of neutron stars** is so extreme that rules of nuclear physics may change leading to the formation of **quark matter**.

Structure of Matter




Quarks

- **Building blocks** of other particles.
- Confined particles **never found in isolation**.
- The energy spent to separate quarks gives rise to new quarks.



Figure: Inseparability of quarks in spite of spending more energy.

- 
- There are six types of quarks known as **up**, **down**, **strange**, **charm**, **top** and **bottom**.
 - **Up** and **down** quarks have the lowest masses of all quarks and are generally **stable**.
 - **Strange**, **charm**, **bottom** and **top** quarks can only be produced in **high energy collisions**.

Quark Star

- A hypothetical compact star.
- Protons and neutrons **deconfine** in the core of a neutron star due to **high temperature** and **extreme pressure** leading to a **bath of quarks**.
- Density is much **higher** than a **neutron star**.
- Masses of quark stars lie between **3 to 5 solar masses**.



Properties of Compact Objects

Energy-Momentum Tensor

- Perfect fluid

$$T_{\gamma\delta} = (\rho + p)u_{\gamma}u_{\delta} + pg_{\gamma\delta}.$$

- Anisotropic fluid

$$T_{\gamma\delta} = (\rho + p_{\perp})u_{\gamma}u_{\delta} - p_{\perp}g_{\gamma\delta} + (p_r - p_{\perp})u_{\gamma}u_{\delta}.$$

Equation of State

- The relation between **state determinants** (density, pressure, etc.).
- Characterizes the **state of matter** under a given set of physical conditions.

MIT Bag Model

The equation of state is given as

$$p_r = \frac{1}{3} (\rho - 4\mathfrak{B}).$$

Different values of the bag constant represent different scenarios.

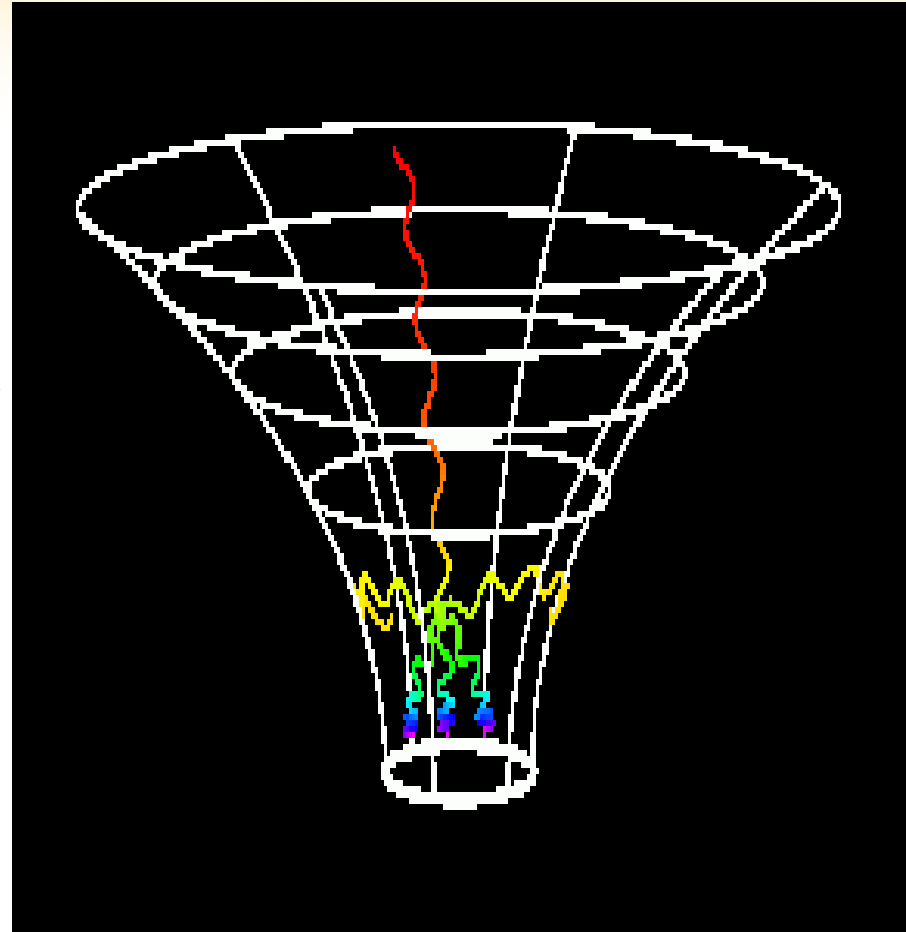
The Bag Constant

- The range of \mathcal{B} for massless strange quarks is $58.9-91.5 \text{ MeV}/\text{fm}^3$ [Farhi, E. and Jaffe, R.L.: Phys. Rev. D **30**(1984)2379].
- For massive quarks, \mathcal{B} lies within the range $56-78 \text{ MeV}/\text{fm}^3$ [Stergioulas, N.: Living Rev. Relativ. **6**(2003)3].

- However, larger values have also been suggested for the bag constant. Xu et al. [*Chin. J. Astron. Astrophys.* **3**(2003)33.] proposed that for an MIT bag model with $\mathcal{B} = 60 \text{ MeV}/\text{fm}^3$, $110 \text{ MeV}/\text{fm}^3$, the star **LMXB EXO 0748-676** can be treated as a candidate for strange star.
- Experimental data of **CERN-SPS** and **RHIC** also allows a **wider range** of values for the bag constant [*Rahaman, F. et al.: Eur. Phys. J. C* **72**(2012)2071; *Kalam, M. et al.: Int. J. Theor. Phys.* **52**(2013)3319].

Gravitational Redshift

If the **energy** of the photon decreases, the **frequency** also decreases. This corresponds to an **increase in the wavelength** of the photon, or a shift to the red end of the electromagnetic spectrum – hence the name: **gravitational redshift**.






The gravitational redshift of a dense compact object is calculated as

$$Z = \frac{1}{\sqrt{1 - 2u(r)}} - 1,$$

where $u(r) = \frac{m}{r}$ is the compactness factor.



Buchdahl [Phys. Rev. D **116**(1959)1027.] calculated the upper limit of mass to radius ratio as

$$\frac{m}{r} < \frac{4}{9},$$

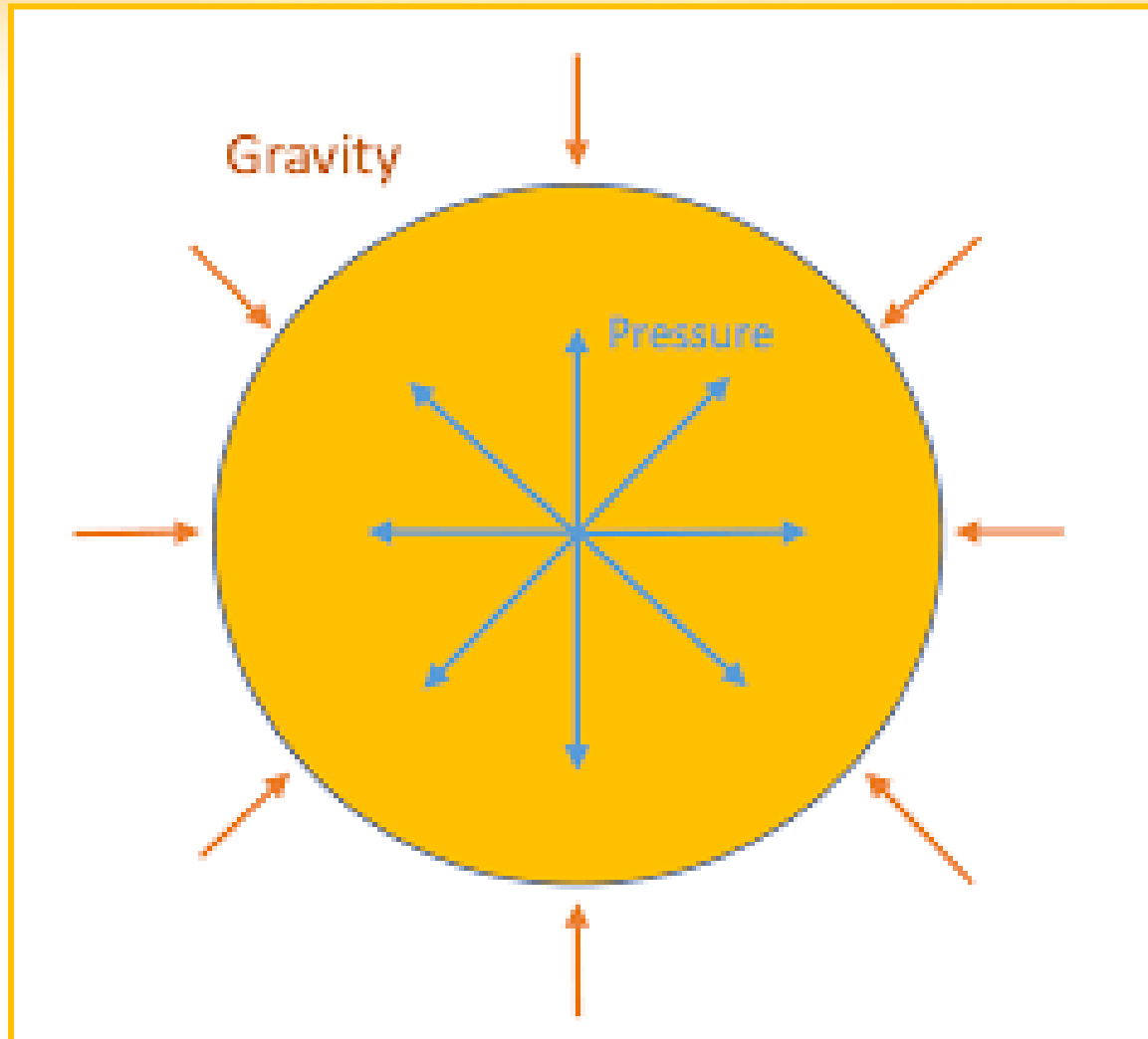
which implies that the upper limit of gravitational redshift is [Ivanov, B.V.: Phys. Rev. D **65**(2002)104011.]

$$Z < 5.211.$$

Equilibrium

A condition of a system when neither its **state of motion** nor its **internal energy** changes under the action of external forces.

Stellar Equilibrium



Stability

In a stable system, a small disturbance will fade away, i.e., the system will stay in, or return to, the equilibrium position.

Checking Stability


- Causality Condition
- Herrera's Cracking Approach
- Adiabatic Index

Causality Condition

The speed of sound in a medium depends on how quickly vibrational energy can be transferred through the medium. For a stable structure, the speed of sound must be less than the speed of light.

Herrera's Cracking Approach

Cracking appears whenever the radial force directed inward in the inner part of the sphere changes its sign beyond some value of the radial coordinate [Herrera, L.: Phys. Lett. A **165**(1992)206].



Based on the concept of cracking and causality condition, Abreu et al. [Class. Quantum Gravit. **24(2007)4631.**] obtained another condition of stability as

$$0 < |v_{\perp}^2 - v_r^2| < 1.$$

Junction Conditions

The matching of matter to empty space at the boundary of a star must be smooth. For this purpose, the following conditions must be satisfied at the hypersurface (Σ)

$$[ds^2_-]_{\Sigma} = [ds^2_+]_{\Sigma}, \quad [K_{ij-}]_{\Sigma} = [K_{ij+}]_{\Sigma}.$$



Self-interacting Brans-Dicke Theory

Mach's Principle

The inertial forces observed locally in an accelerated laboratory may be interpreted as gravitational effects having their origin in distant matter accelerated relative to laboratory.

Theory of General Relativity

$$G_{\gamma\delta} = \mathfrak{R}_{\gamma\delta} - \frac{1}{2}\mathfrak{R}g_{\gamma\delta} + \Lambda g_{\gamma\delta} = \frac{8\pi G}{c^4}T_{\gamma\delta}.$$



Dirac's Large Numbers Hypothesis

Relationship between ratios of **size scales** in the universe to that of **force scales** which yield very large dimensionless numbers.

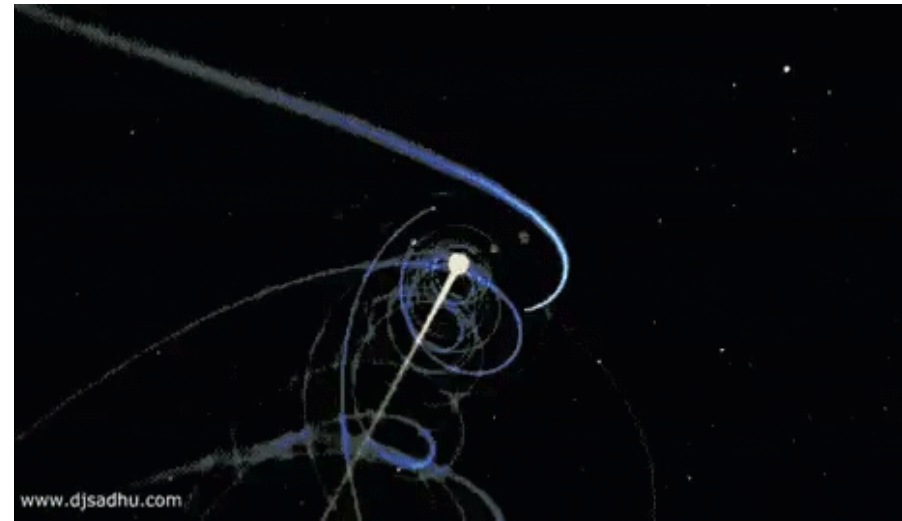


Relation between inertial forces and the overall mass distribution holds if

$$\frac{GM}{R} \approx 1.$$

The Expanding Universe

In 1929, Edwin Hubble discovered that the farther a galaxy is the faster it recedes from us.



M → Mass of the **visible** universe.

R → Radius of the **observable** universe.

Hence, G is not a constant but varies from time to time.

Brans-Dicke Theory

In 1961, Brans and Dicke introduced a scalar-tensor theory by representing the reciprocal of varying gravitational constant through a scalar field Φ . The scalar field is coupled to matter as well as gravity through a **coupling parameter** (ω_{BD}).

Self-interacting Brans-Dicke Theory

- Low values of **coupling parameter** are used to describe cosmic inflation [Weinberg, E.J.: Phys. Rev. D **40**(1989)3950].
- For weak field situations, the value of **coupling parameter** must be greater than **40,000** [Will C.M.: Living Rev. Rel. **4**(2001)4.] and deviations from general relativity are insignificant.

Self-interacting Brans-Dicke Theory

The action of self-interacting Brans-Dicke (SBD) theory is

$$S = \int \sqrt{-g} \left(\mathcal{R}_\zeta - \frac{\omega_{BD}}{\zeta} \partial_\gamma \zeta \partial_\delta \zeta - V(\zeta) + L_m \right) d^4x.$$

Field Equations:

$$G_{\gamma\delta} = T_{\gamma\delta}^{(\text{eff})} = \frac{1}{\zeta} (T_{\gamma\delta}^{(m)} + T_{\gamma\delta}^{\zeta}),$$

Wave Equation:

$$\square\zeta = \frac{T^{(m)}}{3+2\omega_{BD}} + \frac{1}{3+2\omega_{BD}} \left(\zeta \frac{dV(\zeta)}{d\zeta} - 2V(\zeta) \right),$$

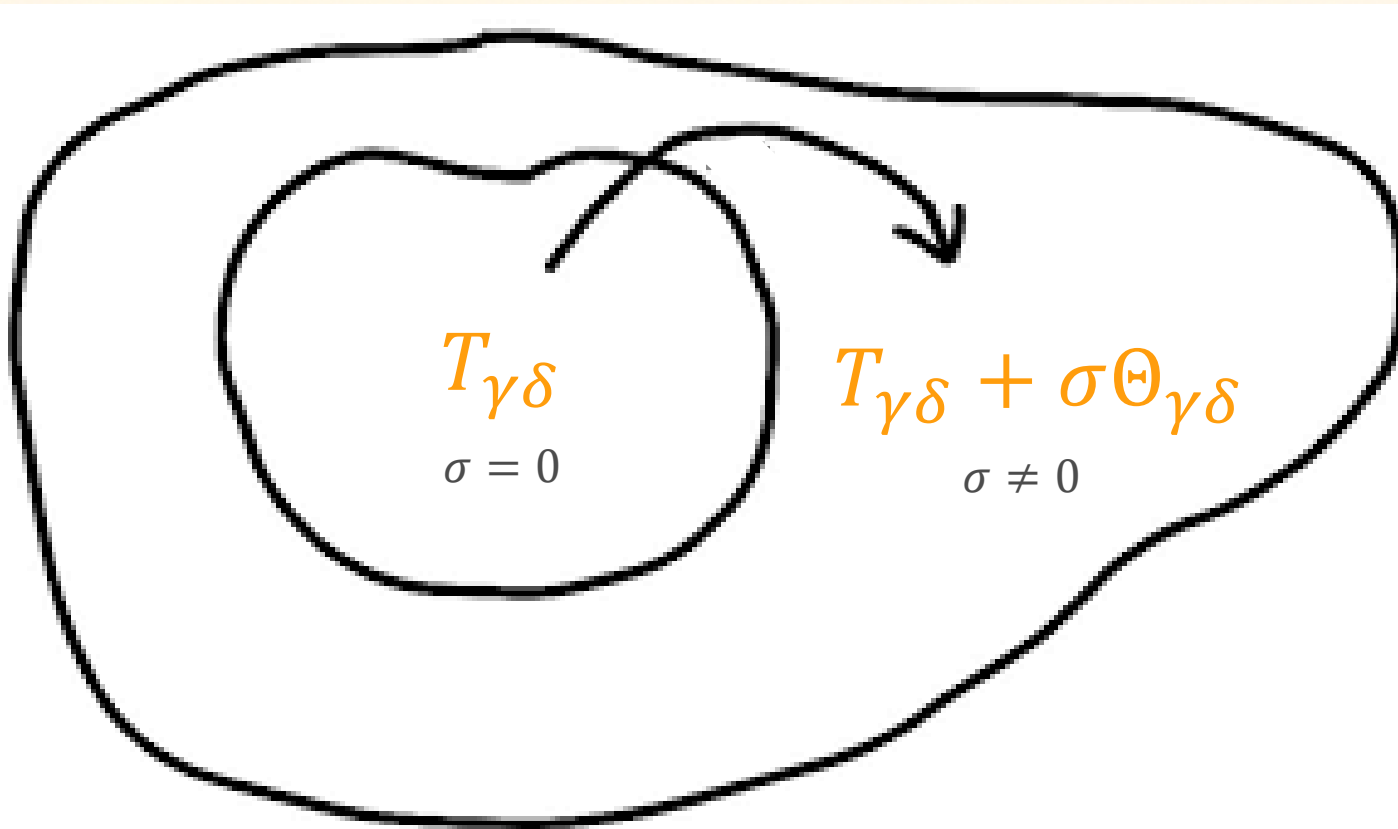
where

$$T_{\gamma\delta}^{\zeta} = \zeta_{,\gamma;\delta} - g_{\gamma\delta} \square\zeta + \frac{\omega_{BD}}{\zeta} \left(\zeta_{,\gamma}\zeta_{,\delta} - \frac{g_{\gamma\delta}\zeta_{\alpha}\zeta^{\alpha}}{2} \right) - \frac{V(\zeta)}{2} g_{\gamma\delta}.$$



Gravitational Decoupling Scheme

Gravitational Decoupling



Scheme

Add a new gravitational source in the original energy-momentum tensor.

Deform the radial metric potential to decouple the field equations into two sets.

- The first set corresponds to the original source.
- The second set relates to the new source.

Assume a known solution for the first set.
Find a solution of the second set.

Combine solutions of both sets to obtain a new solution.

Minimal Geometric Deformation

- It only deforms the **radial metric potential** by leaving temporal component unchanged.
- It works as long as the **interaction** between the matter sources is purely **gravitational**.

Physical Acceptability Conditions

- The **metric co-efficients** must be positive and monotonically increasing.
- The physical parameters (ρ , p_r , p_{\perp}) must be maximum at the center and monotonically decreasing towards the boundary.
- Radial pressure must be **zero at the boundary**.

- The anisotropy ($\Delta = p_{\perp} - p_r$) must be zero at the center.
- Following energy conditions must be satisfied.
 - Weak Energy Condition: $\rho + p_r \geq 0, \rho + p_{\perp} \geq 0$.
 - Null Energy Condition: $\rho \geq 0, \rho + p_r \geq 0, \rho + p_{\perp} \geq 0$.
 - Strong Energy Condition: $\rho + p_r \geq 0, \rho + p_r + 2p_{\perp} \geq 0$.
 - Dominant Energy Condition: $\rho - p_r \geq 0, \rho + p_{\perp} \geq 0$.



Decoupled Solutions in Self-interacting Brans-Dicke Theory

Spherical Spacetime

The line element describing a static sphere is given by

$$ds^2 = e^{\phi(r)} dt^2 - e^{\psi(r)} dr^2 - r^2 d\theta^2 - r^2 \sin^2 \theta d\varphi^2.$$

The matter distribution describing the internal configuration of the spherical structure is

$$T_{\gamma\delta}^{(\text{eff})} = \frac{1}{\zeta} (T_{\gamma\delta}^{(m)} + \sigma \Theta_{\gamma\delta} + T_{\gamma\delta}^{\zeta}).$$

The field equations are obtained as

$$\frac{1}{r^2} - e^{-\psi} \left(\frac{1}{r^2} - \frac{\psi'}{r} \right) = \frac{1}{\varsigma} (\rho + \sigma \Theta_0^0 + T_0^{0\varsigma}),$$

$$-\frac{1}{r^2} + e^{-\psi} \left(\frac{1}{r^2} + \frac{\phi'}{r} \right) = \frac{1}{\varsigma} (p - \sigma \Theta_1^1 - T_1^{1\varsigma}),$$

$$\frac{e^{-\psi}}{4} \left(2\phi'' + \phi'^2 - \psi'\phi' + 2\frac{\phi' - \psi'}{r} \right) = \frac{1}{\varsigma} (p - \sigma \Theta_2^2 - T_2^{2\varsigma}),$$

where

$$T_0^{0\zeta} = e^{-\psi} \left[\zeta'' + \left(\frac{2}{r} - \frac{\psi'}{2} \right) \zeta' + \frac{\omega_{BD}}{2\zeta} \zeta'^2 - e^\psi \frac{V(\zeta)}{2} \right],$$

$$T_1^{1\zeta} = e^{-\psi} \left[\left(\frac{2}{r} + \frac{\phi'}{2} \right) \zeta' - \frac{\omega_{BD}}{2\zeta} \zeta'^2 - e^\psi \frac{V(\zeta)}{2} \right],$$

$$T_2^{2\zeta} = e^{-\psi} \left[\zeta'' + \left(\frac{1}{r} - \frac{\psi'}{2} + \frac{\phi'}{2} \right) \zeta' + \frac{\omega_{BD}}{2\zeta} \zeta'^2 - e^\psi \frac{V(\zeta)}{2} \right].$$

The wave equation reads

$$\begin{aligned}\square_{\zeta} &= -e^{-\psi} \left[\left(\frac{2}{r} - \frac{\psi'}{2} + \frac{\phi'}{2} \right) \zeta' + \zeta'' \right] \\ &= \frac{1}{3 + 2\omega_{BD}} \left[T^{(m)} + \Theta + \left(\zeta \frac{dV(\zeta)}{d\zeta} - 2V(\zeta) \right) \right].\end{aligned}$$

The potential function is chosen as

$$V(\zeta) = \frac{1}{2} m_{\zeta}^2 \zeta^2.$$

Transformations

Apply the MGD technique through the transformation

$$e^{-\psi(r)} \mapsto \lambda(r) + \sigma\nu(r),$$

where $\nu(r)$ is the deformation function that governs the translation in the radial metric component. The temporal metric potential remains unchanged.

Decoupling

The first set corresponds to $\sigma = 0$ and exclusively describes the isotropic configuration as

$$\begin{aligned}\rho &= -\frac{1}{2r^2\zeta(r)}[r^2\omega\lambda(r)\zeta'^2(r) - r^2\zeta(r)V(\zeta) + r\zeta(r)(r\lambda'(r)\zeta'(r) + 2r\lambda(r)\zeta''(r) \\ &+ 4\lambda(r)\zeta'(r)) + 2\zeta^2(r)(r\lambda'(r) + \lambda(r) - 1)], \\ p &= \frac{1}{r^2}[\zeta(r)(r\lambda(r)\phi'(r) + \lambda(r) - 1)] + \frac{1}{2r\zeta(r)}[\lambda(r)\zeta'(r)(\zeta(r)(r\phi'(r) + 4) \\ &- r\omega_{BDS}\zeta'(r))] - \frac{V(\zeta)}{2}, \\ p &= \frac{1}{4r\zeta(r)}[\zeta(r)\lambda'(r)(\zeta(r)(r\phi'(r) + 2) + 2r\zeta'(r)) + \lambda(r)(2\zeta(r)\zeta'(r) \\ &\times ((r\phi'(r) + 2) + 2r\zeta''(r)) + \zeta^2(r)(2r\phi''(r) + r\phi'^2(r) + 2\phi'(r)) \\ &+ 2r\omega_{BDS}\zeta'^2(r)) - 2r\zeta(r)V(\zeta)].\end{aligned}$$

The second set containing evolution equations for the anisotropic source is given as

$$\begin{aligned}
 \Theta_0^0 &= \frac{-1}{2r^2\zeta(r)} [r\zeta(r)\nu'(r)(r\zeta'(r) + 2\zeta(r)) + \nu(r)(r^2\omega_{BD}\zeta'^2(r) + 2r\zeta(r) \\
 &\times (r\zeta''(r) + 2\zeta'(r)) + 2\zeta^2(r))], \\
 \Theta_1^1 &= \frac{-1}{2r^2\zeta(r)} [\nu(r)(-r^2\omega_{BD}\zeta'(r)^2 + r\zeta(r)(r\phi'(r) + 4)\zeta'(r) + 2\zeta^2(r) \\
 &\times (r\phi'(r) + 1))], \\
 \Theta_2^2 &= \frac{-1}{4\zeta(r)} [2\zeta(r)(r\nu'(r)\zeta'(r) + \nu(r)((r\phi'(r) + 2)\zeta'(r) + 2r\zeta''(r))) \\
 &+ \zeta^2(r)(\nu'(r)(r\phi'(r) + 2) + \nu(r)(2r\phi''(r) + r\phi'^2(r) + 2\phi'(r))) \\
 &+ 2r\omega_{BD}\nu(r)\zeta'^2(r)].
 \end{aligned}$$

Conservation of Mass and Energy

The conservation of isotropic matter distribution is represented by the equation

$$T_1^{1'(\text{eff})} - \frac{\phi'(r)}{2} (T_0^{0(\text{eff})} - T_1^{1(\text{eff})}) = 0.$$

Whereas the divergence of the additional source leads to

$$\Theta_1^{1'(\text{eff})} - \frac{\phi'(r)}{2} (\Theta_0^{0(\text{eff})} - \Theta_1^{1(\text{eff})}) - \frac{2}{r} (\Theta_2^{2(\text{eff})} - \Theta_1^{1(\text{eff})}) = 0,$$

$$\begin{aligned}
\Theta_0^{0(\text{eff})} &= \frac{1}{\varsigma} \left(\Theta_0^0 + \frac{1}{2} \nu'(r) \varsigma'(r) + \nu(r) \varsigma''(r) + \frac{\omega_{BD} \nu(r) \varsigma'^2(r)}{2\varsigma(r)} + \frac{2\nu(r) \varsigma'(r)}{r} \right), \\
\Theta_1^{1(\text{eff})} &= \frac{1}{\varsigma} \left(\Theta_1^1 + \frac{1}{2} \nu(r) \phi'(r) \varsigma'(r) - \frac{\omega_{BD} \nu(r) \varsigma'^2(r)}{2\varsigma(r)} + \frac{2\nu(r) \varsigma'(r)}{r} \right), \\
\Theta_2^{2(\text{eff})} &= \frac{1}{\varsigma} \left(\Theta_2^2 + \frac{1}{2} \nu'(r) \varsigma'(r) + \frac{1}{2} \nu(r) \phi'(r) \varsigma'(r) + \nu(r) \varsigma''(r) \right. \\
&\quad \left. + \frac{\omega_{BD} \nu(r) \varsigma'^2(r)}{2\varsigma(r)} + \frac{\nu(r) \varsigma'(r)}{r} \right).
\end{aligned}$$

Isotropic Solutions

We extend Tolman V solution [Phys. Rev. **55**(1939)364.]

to anisotropic domain. Tolman V spacetime is defined as

$$ds^2 = B^2 r^{2n} dt^2 - \left(\frac{1 + 2n - n^2}{1 - (1 + 2n - n^2) \left(\frac{r}{F}\right)^W} \right) dr^2 - r^2 d\theta^2 - r^2 \sin^2 \theta d\varphi^2,$$

where n , F and B are unknown constants with W
 $= \frac{2(1+2n-n^2)}{1+n}$.

The energy density and pressure of the anisotropic analogue of Tolman V are expressed as

$$\begin{aligned}
 \rho &= \frac{-1}{2r^2\zeta} \left(r\zeta \left(r\zeta' \left(\sigma\nu'(r) + \frac{\zeta_1}{r} \right) + 2\sigma\nu(r) (r\zeta'' + 2\zeta') + 2\zeta_2 (r\zeta'' \right. \right. \\
 &+ \left. \left. 2\zeta') \right) + 2\zeta^2 (\sigma r\nu'(r) + \sigma\nu(r) + \zeta_1 + \zeta_2 - 1) + r^2\omega_{BD}\zeta'^2 (\sigma\nu(r) \right. \\
 &+ \left. \zeta_2) - r^2\zeta V(\zeta) \right), \\
 p_r &= \frac{\zeta}{r^2} (\nu(r)(\sigma + 2\sigma n) + \zeta_2(2n + 1) - 1) + \frac{\zeta' (2(n + 2)\zeta - r\omega_{BD}\zeta')}{2r\zeta} \\
 &\times (\sigma\nu(r) + \zeta_2) - \frac{V(\zeta)}{2},
 \end{aligned}$$

$$\begin{aligned}
p_{\perp} &= \frac{\zeta}{2r^2} \left(\sigma(n+1)r\nu'(r) + 2\sigma n^2\nu(r) + \frac{1}{\zeta_3^2}((n-2)n-1)(2n-n^2+1) \right. \\
&\times \left. (2n^2 - (n+1)W) \left(\frac{r}{F} \right)^W - 2n^2 \right) + (\sigma\nu(r) + \zeta_2) \left(\frac{\zeta'}{2} \right. \\
&\times \left. \left(\frac{\sigma\nu'(r) + \frac{\zeta_1}{r}}{\sigma\nu(r) + \zeta_2} + \frac{2n}{r} + \frac{2}{r} \right) + \zeta'' + \frac{\omega_{BD}\zeta'^2}{2\zeta} \right) - \frac{V(\zeta)}{2},
\end{aligned}$$

where $\zeta_1 = \frac{(n^2-2n-1)^2 W \left(\frac{r}{F}\right)^W}{(\zeta_3)^2}$, $\zeta_2 = \frac{-n^2+2n+1}{\zeta_3}$ and $\zeta_3 = \left((n^2-2n-1) \left(\frac{r}{F}\right)^W + 1 \right)$.

The unknown constants are evaluated through matching with Schwarzschild spacetime as

$$\begin{aligned} B &= \frac{\sqrt{M} R^{\frac{R}{4M-2R}}}{\sqrt{-\frac{M}{2M-R}}}, \\ n &= \frac{M}{R-2M}, \\ W &= -\frac{2(M^2 + 2MR - R^2)}{2M^2 - 3MR + R^2}, \\ F &= R \left(\frac{M^2(R-2M)}{R(-M^2 - 2MR + R^2)} \right)^{-\frac{1}{W}}, \end{aligned}$$

$$\omega_{BD} = \frac{2M - R}{8M^2((n - 2)n - 1)} \left(-((n - 2)n - 1)(2M - R) \left(\frac{R}{F}\right)^W (m_\zeta R \right. \\ \times (2M - R) - 4) - 4m_\zeta M^2 R + 4m_\zeta M R^2 - m_\zeta R^3 + 8Mn^3 \\ \left. - 24Mn^2 + 8Mn + 16M - 8n^3 R + 12n^2 R + 16nR) \right).$$

MIT Bag Model

In order to determine the deformation function, we apply the bag model on the system which yields the following differential equation

$$\begin{aligned} & (\sigma r \nu'(r) \zeta' + \sigma \nu(r) (2(3n + 8) \zeta' + 2r \zeta'')) + 2\zeta_2 r \zeta'' + \zeta_1 \zeta' + 6n \zeta_2 \zeta' \\ & + 16\zeta_2 \zeta' - 4rV(\zeta) + 8r\mathcal{B} + \frac{2\zeta}{r} (\sigma r \nu'(r) + \sigma(6n + 4)\nu(r) + \zeta_1 \\ & + (6n + 4)\zeta_2 - 4) - 2r^2 \omega_{BD} \zeta'^2 (\sigma \nu(r) + \zeta_2) = 0, \end{aligned}$$

which is numerically solved along with the wave equation subject to central conditions ($\zeta(0) = 0.2$, $\zeta'(0) = 0$ and $\nu(0) = \nu_c$) for three stars: PSR J1614-2230, Her X1 and 4U 1608-52

Case I: Linear Equation of State

Table 1: Values of different parameters corresponding to stellar candidates for $m_\zeta = 0.001$ and $\mathcal{B} = 60 \text{ MeV}/\text{fm}^3$.

| | PSR J1614-2230 | Her X-1 | 4U 1608-52 |
|------------------------|----------------|---------|------------|
| $M (M_\odot)$ | 1.97 | 0.88 | 1.74 |
| $R (km)$ | 13 | 7.7 | 9.3 |
| ω_{BD} | 9.750 | 15.353 | 6.593 |
| $\nu_c (\sigma = 0.2)$ | -5.1 | -3.6 | -6.8 |
| $\nu_c (\sigma = 0.9)$ | -1.132 | -0.8 | -1.5 |



Extended Tolman V Solution

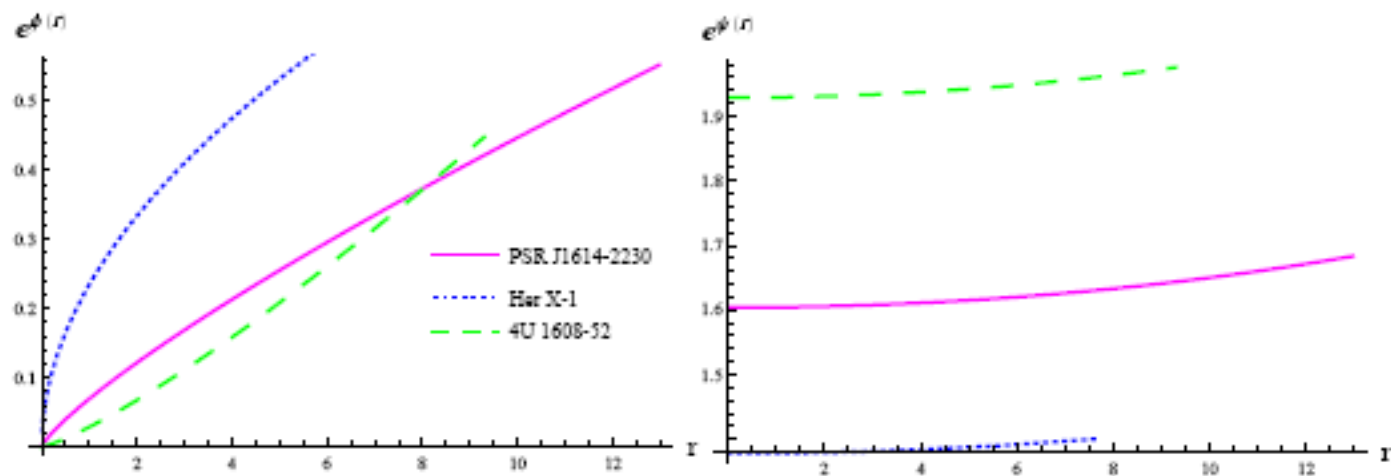


Figure 1: Plots of temporal and radial metric components of anisotropic Tolman V solution for $\sigma = 0.2$.

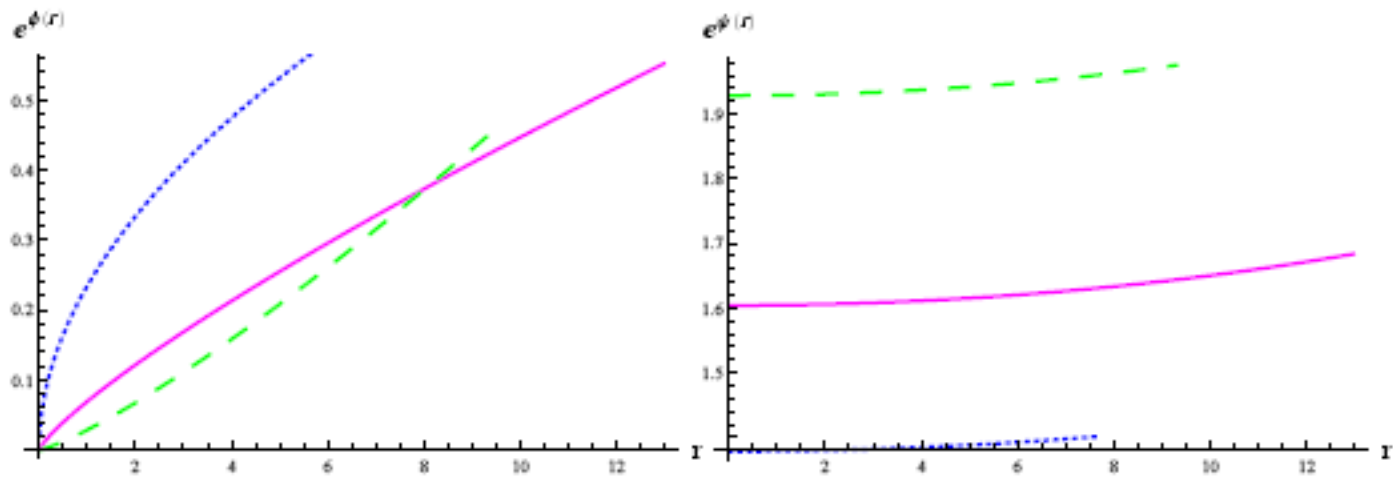


Figure 2: Plots of temporal and radial metric components of anisotropic Tolman V solution for $\sigma = 0.9$.

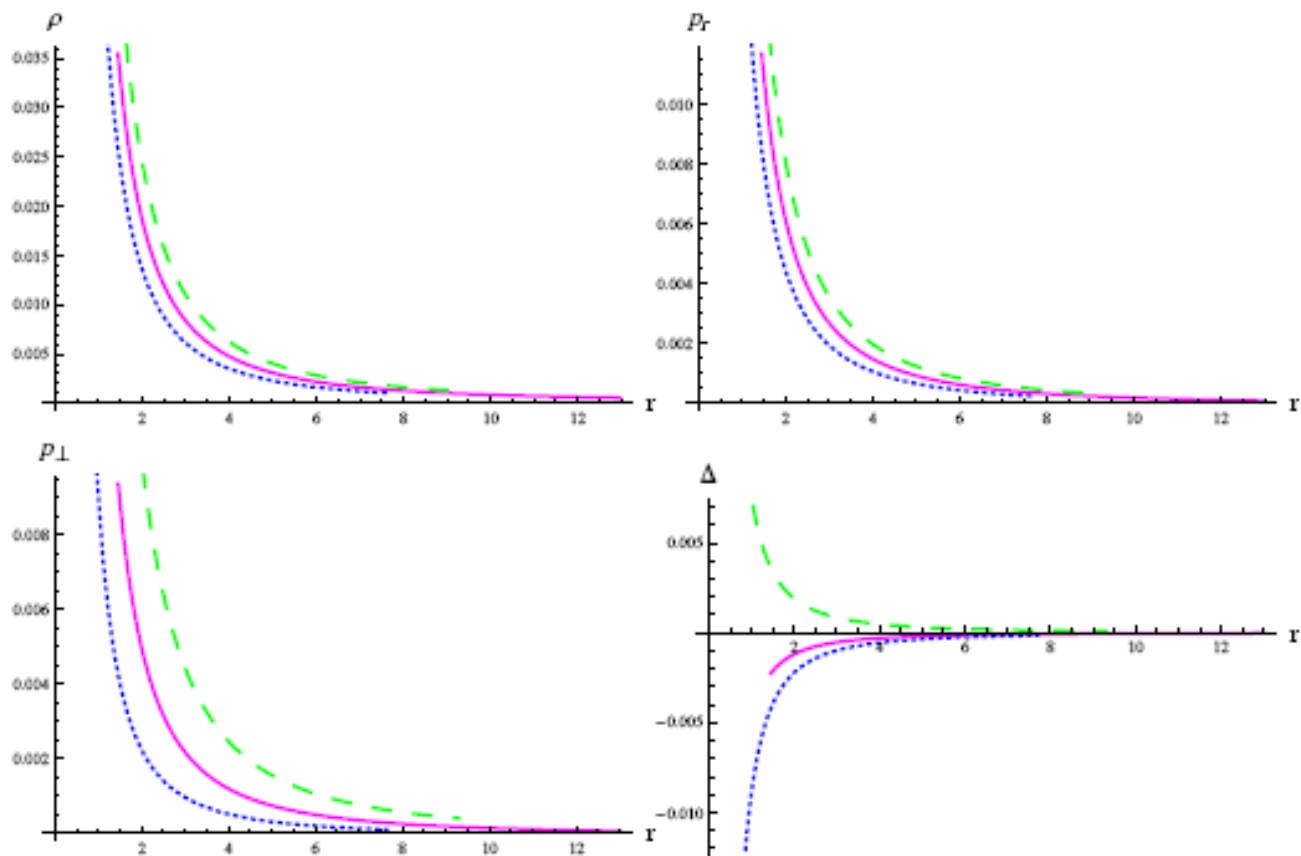


Figure 3: Plots of ρ , p_r , p_{\perp} (in km^{-2}) and Δ of anisotropic Tolman V solution for $\sigma = 0.2$.

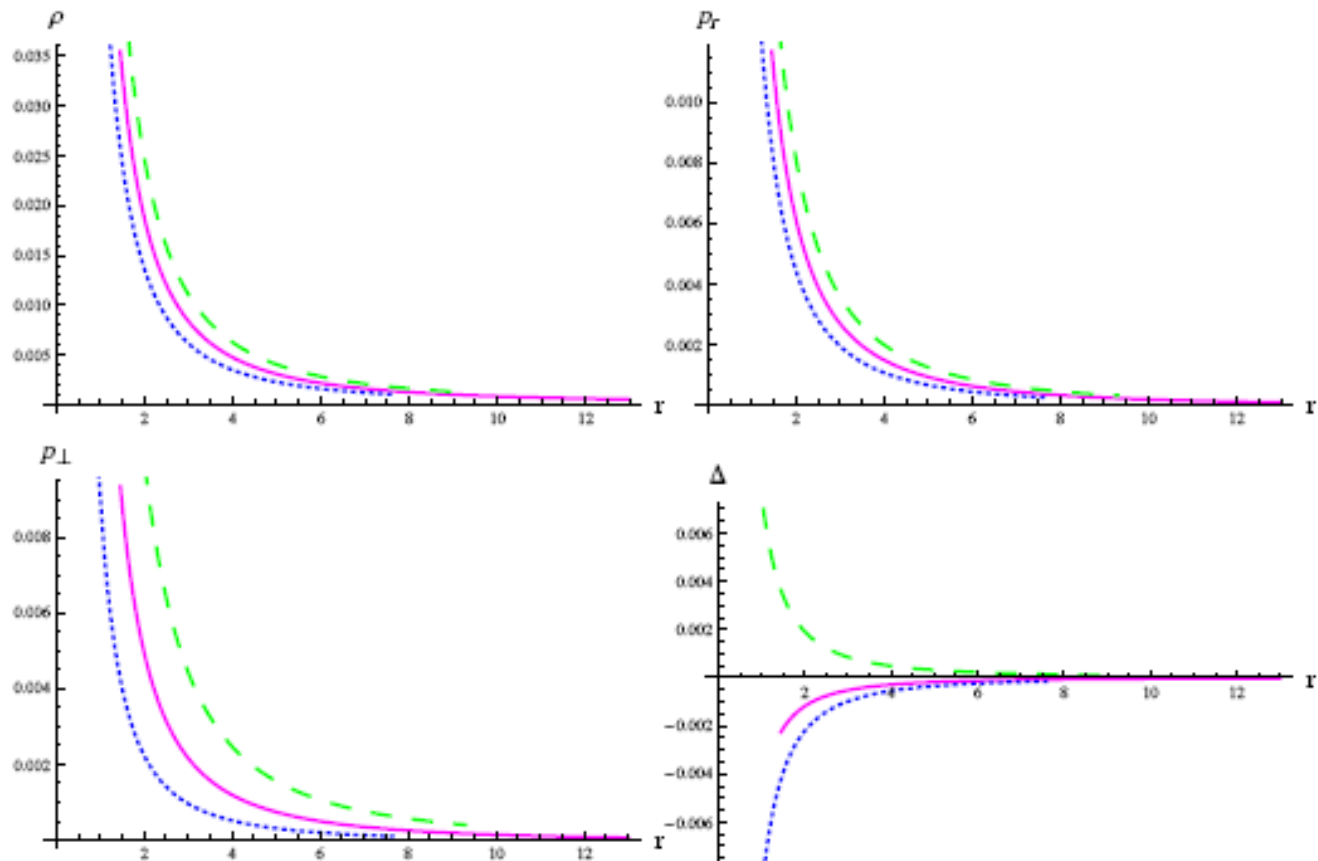


Figure 4: Plots of ρ , p_r , p_{\perp} (in km^{-2}) and Δ of anisotropic Tolman V solution for $\sigma = 0.9$.

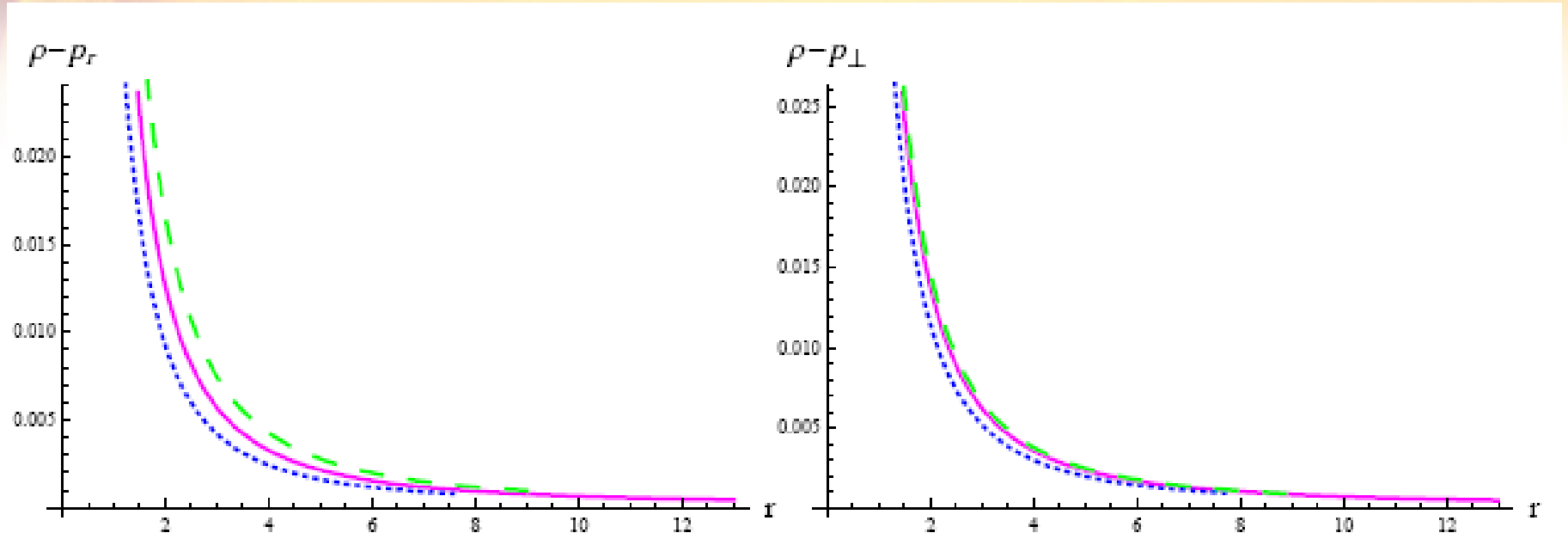


Figure 5: DEC for extended Tolman V solution for $\sigma = 0.2$.

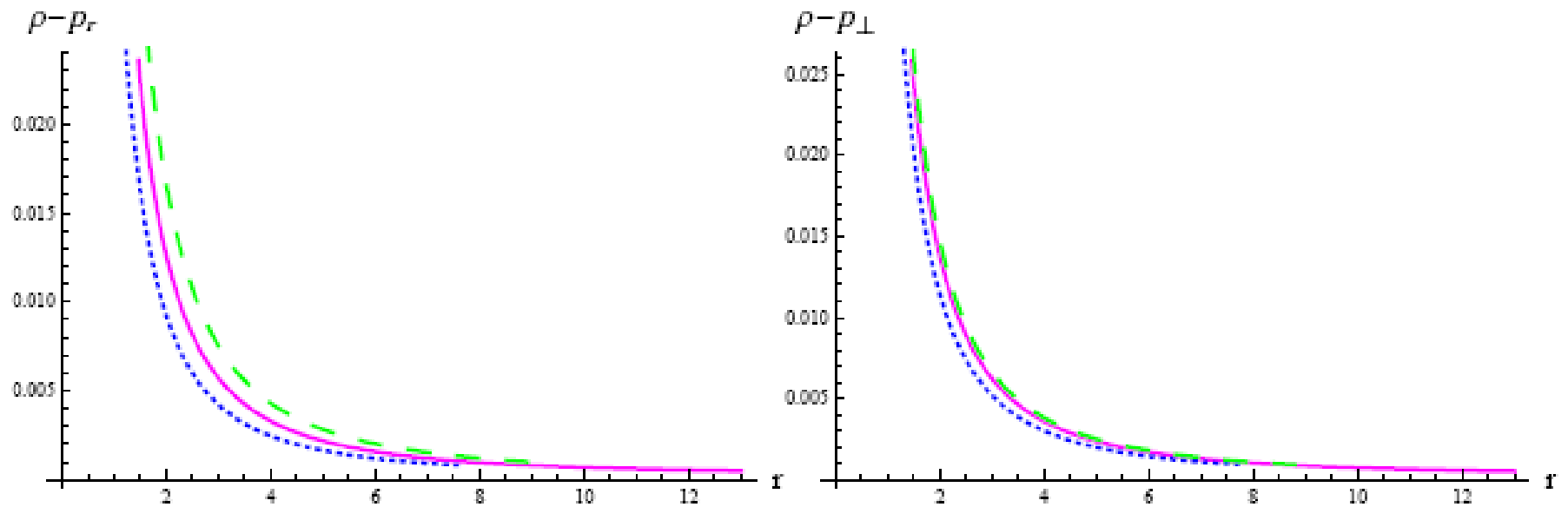


Figure 6: DEC for extended Tolman V solution for $\sigma = 0.9$.

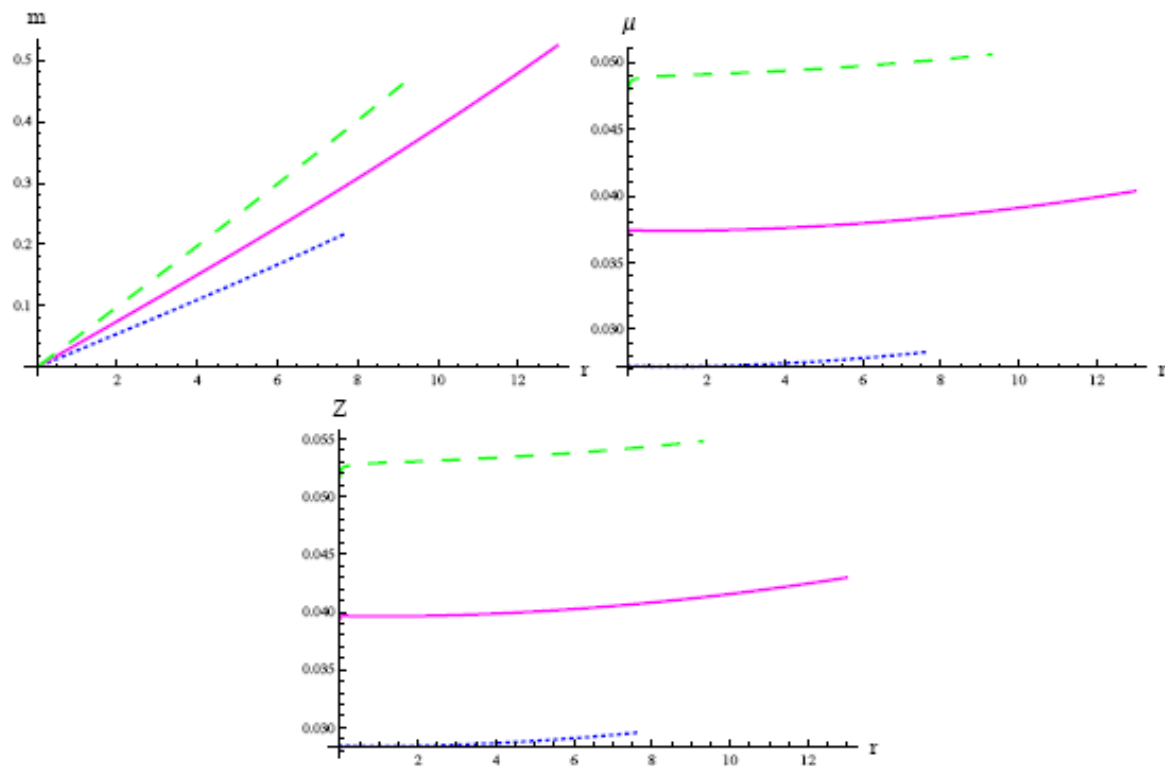


Figure 7: Plots of m , μ and Z corresponding to anisotropic Tolman V solution for $\sigma = 0.2$.

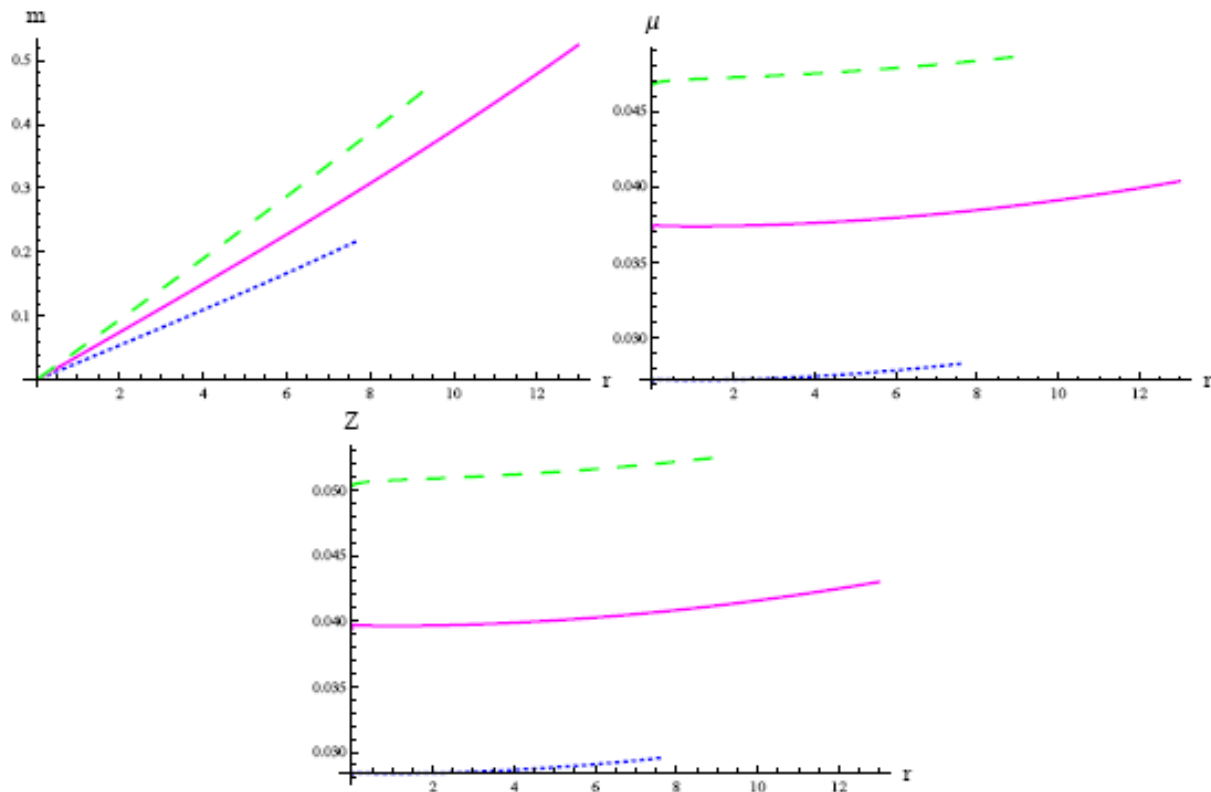


Figure 8: Plots of m , μ and Z corresponding to anisotropic Tolman V solution for $\sigma = 0.9$.

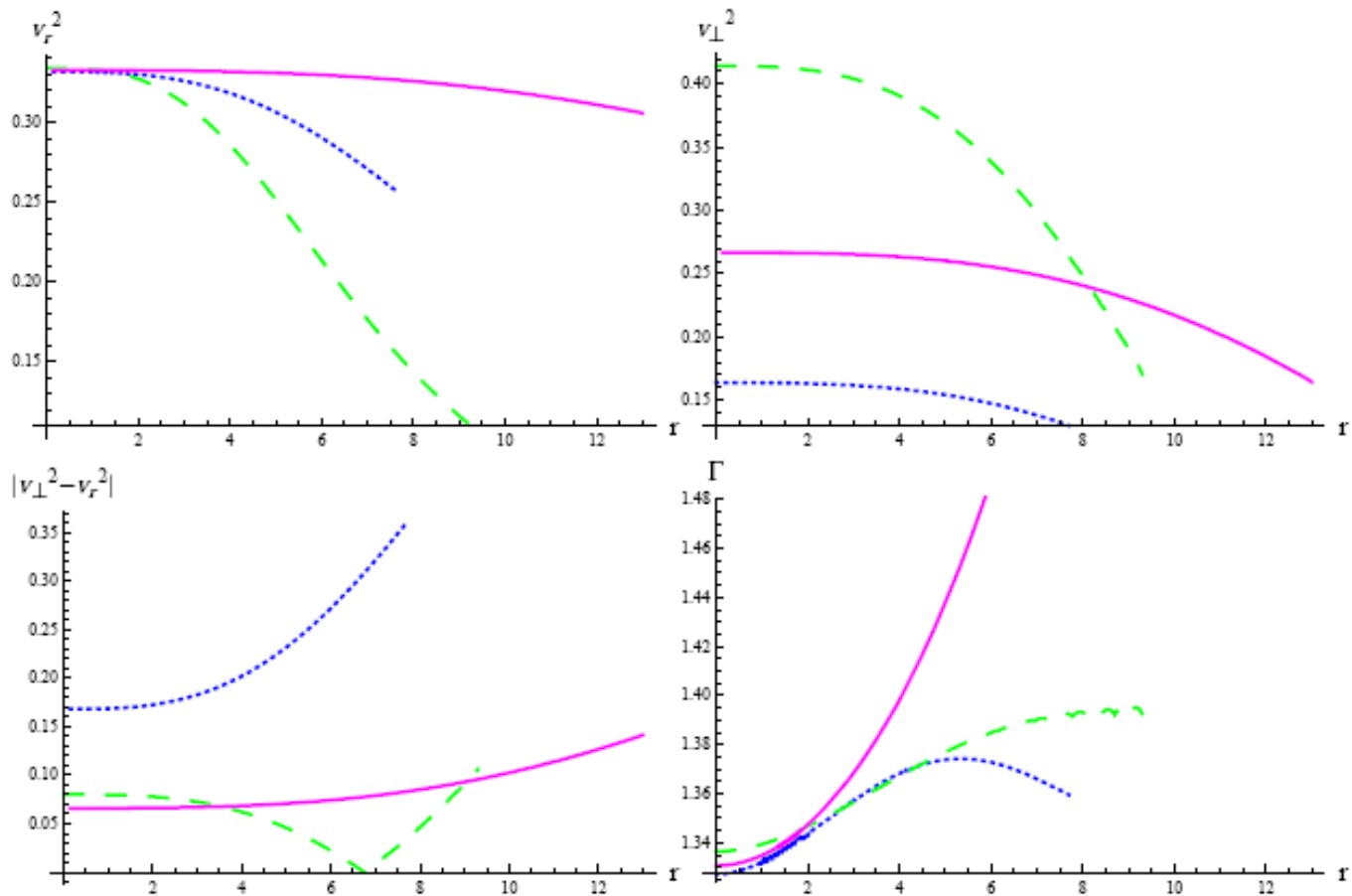


Figure 9: Plots of radial/tangential velocities, $|v_{\perp}^2 - v_r^2|$ and adiabatic index of extended Tolman V solution for $\sigma = 0.2$.

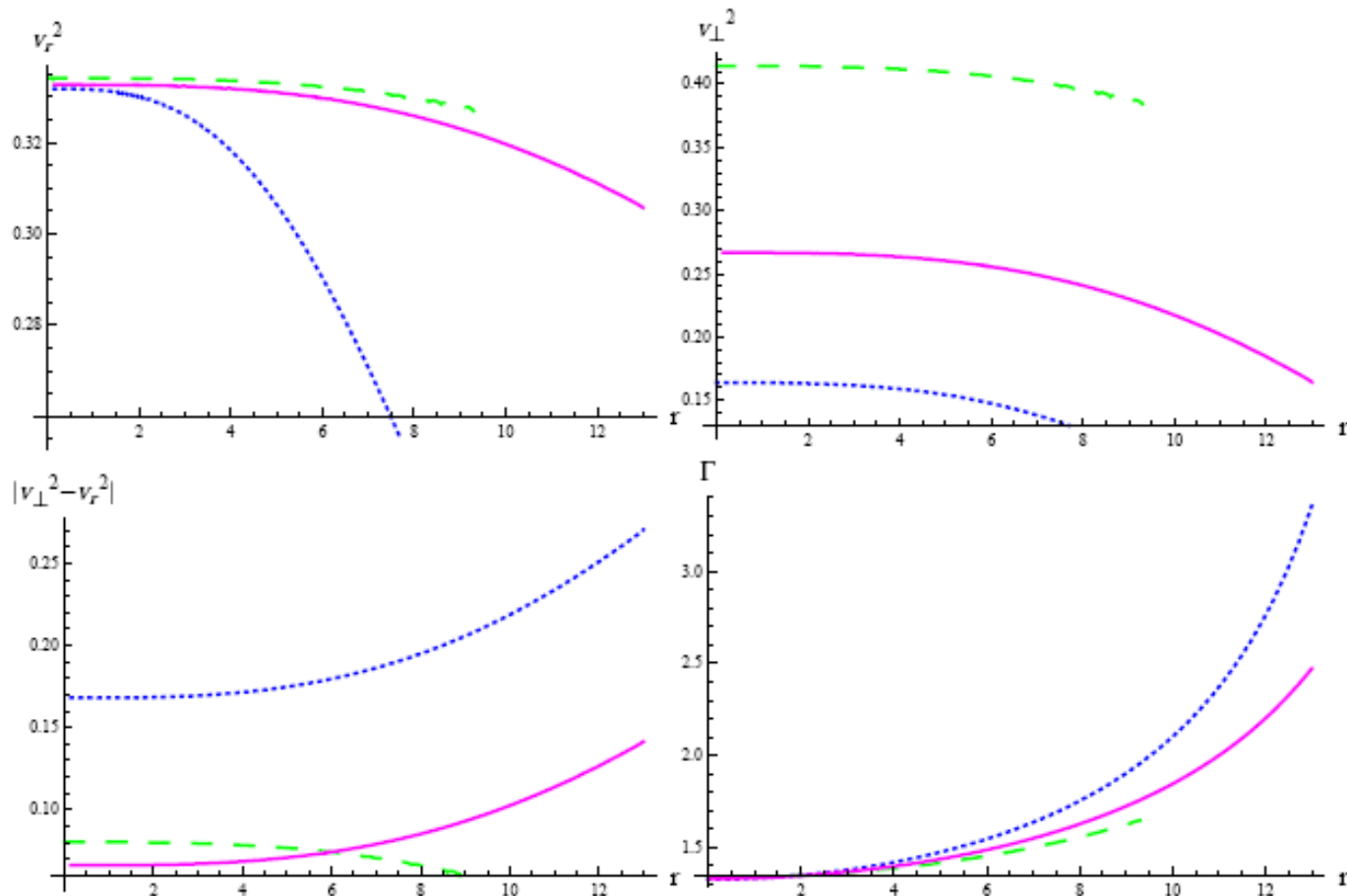



Figure 10: Plots of radial/tangential velocities, $|v_{\perp}^2 - v_r^2|$ and adiabatic index of extended Tolman V solution for $\sigma = 0.9$.



Concluding Remarks



We have formulated an **anisotropic** model for **strange quark star** through **MGD** technique in **SBD gravity**.

- Anisotropy has been induced in the isotropic matter configuration by means of an **additional source**.
- The two sources (seed and additional) have been decoupled through a **linear transformation of the radial metric component**.
- We have considered **Tolman V spacetime** as a solution for the array corresponding to the **isotropic** source.
- The second system has been solved by imposing **MIT bag model** on state variables.

- We have numerically evaluated the wave equation for $V(\zeta) = \frac{1}{2}m_\zeta^2 \zeta^2$, $m_\zeta = 0.001$ and $\sigma = 0.2, 0.9$.
- The physical behavior of the extended model has been examined for $\mathfrak{B} = 60 \text{ MeV}/\text{fm}^3$ through energy constraints as well as causality and cracking approaches for the stars Her X-1, PSR J1614-2230 and 4U 1608-52.
- The strange star structure formulated via decoupling is physically realistic and stable in the presence of a massive scalar field.

Thank You